Angiotensin 1-7 as Means to Prevent the Metabolic Syndrome

Lessons From the Fructose-Fed Rat Model

Yonit Marcus,[1,2] Gabi Shefer,[2,3] Keren Sasson,[1] Fortune Kohen,[4] Rona Limor,[2] Orit Pappo,[5] Nava Nevo,[4] Inbal Biton,[6] Michal Bach,[2] Tamara Berkutzki,[6] Matityahu Fridkin,[7] Dafna Benayahu,[3] Yoram Shechter,[1] and Naftali Stern[2,3]

We studied the effects of chronic angiotensin 1-7 (Ang 1-7) treatment in an experimental model of the metabolic syndrome, i.e., rats given high-fructose/low-magnesium diet (HFrD). Rats were fed on HFrD for 24 weeks with and without Ang 1-7 (576 μg/kg/day, s.c., Alzet pumps). After 6 months, Ang 1-7–treated animals had lower body weight (−9.5%), total fat mass (detected by magnetic resonance imaging), and serum triglycerides (−51%), improved glucose tolerance, and better insulin sensitivity. Similar metabolic effects were also evident, albeit in the absence of weight loss, in rats first exposed to HFrD for 5 months and then subjected to short-term (4 weeks) treatment with Ang 1-7. Six months of Ang 1-7 treatment were associated with lower plasma renin activity (−40%) and serum aldosterone (−48%), less hepatosteatatitis, and a reduction in epididymal adipocyte volume. The marked attenuation of macrophage infiltration in white adipose tissue (WAT) was associated with reduced levels of the pP65 protein in the epididymal fat tissue, suggesting less activation of the nuclear factor-κB (NFκB) pathway in Ang 1-7–treated rats. WAT from Ang 1-7–treated rats showed reduced NADPH-stimulated superoxide production. In single muscle fibers (myofibers) harvested and grown ex vivo for 10 days, myofibers from HFrD rats gave rise to 20% less myogenic cells than the Ang 1-7–treated rats. Fully developed adipocytes were present in most HFrD myofiber cultures but entirely absent in cultures from Ang 1-7–treated rats. In summary, Ang 1-7 had an ameliorating effect on insulin resistance, hypertriglyceridemia, fatty liver, obesity, adipositis, and myogenic and adipogenic differentiation in muscle tissue in the HFrD rats. ***Diabetes*** **62:1121–1130, 2013**

From the [1]Department of Biological Chemistry, Weizmann Institute of Science, Rehovot, Israel; the [2]Institute of Endocrinology, Metabolism, and Hypertension, Tel Aviv Sourasky Medical Center, Tel Aviv, Israel; the [3]Sackler Faculty of Medicine, Tel Aviv University, Tel Aviv, Israel; the [4]Department of Biological Regulation, Weizmann Institute of Science, Rehovot, Israel; the [5]Department of Pathology, Hadassah-Hebrew University Medical Center, Jerusalem, Israel; the [6]Department of Veterinary Resources, Weizmann Institute of Science, Rehovot, Israel; and the [7]Department of Organic Chemistry, Weizmann Institute of Science, Rehovot, Israel.

Corresponding author: Naftali Stern, stern@tasmc.health.gov.il.

Received 13 June 2012 and accepted 23 October 2012.

DOI: 10.2337/db12-0792

This article contains Supplementary Data online at http://diabetes.diabetesjournals.org/lookup/suppl/doi:10.2337/db12-0792/-/DC1.

Y.M., Y.S., and N.S. contributed equally to this study.

The metabolic syndrome (MetSyn) encompasses cardiometabolic risk determinants including visceral obesity, insulin resistance, glucose intolerance, dyslipidemia, nonalcoholic fatty liver disease, and hypertension (1). Ectopic fat accumulating in the liver, muscle, and pancreas may play an important role, presumably by releasing adipocytokines, which decrease sensitivity to insulin (2) and promote inflammation (3).

Blockade of the renin-angiotensin system, by inhibiting the formation of angiotensin II (Ang II) with angiotensin-converting enzyme inhibitors or by angiotensin receptor blockers, yields a significant (25%) reduction in the incidence of new-onset type 2 diabetes (4). The renin-angiotensin system may also be involved in hepatic inflammation and fibrogenesis (5) and to adversely affect insulin-mediated glucose uptake in skeletal muscles (6). In cultured myofibers, Ang II was shown to induce insulin resistance via impaired insulin signaling, independent of its vascular effects (7). Skeletal muscles are lost in diabetic patients (8), possibly due to local accumulation of adipocytes that potentially replace muscle cells (9). Moreover, the skeletal muscle stem cells, satellite cells, of obese Zucker rats apparently display increased adipogenic potential (10,11). This may account, at least in part, for the inter- and intramuscular adipocyte accumulation characteristics of obesity and the MetSyn and even the sarcopenia associated with aging.

Angiotensin 1-7 (Ang 1-7) opposes many of the adverse cardiovascular effects of Ang II (12), including hypertension, pregnancy-induced hypertension (preeclampsia), renal disease, heart failure, and cardiac arrhythmia (13–15). The best-studied effects of Ang 1-7 are its vasodilator, blood pressure–lowering, and antiproliferative actions in the cardiovascular system. These effects are apparently mediated through Mas, a specific G protein–coupled receptor for Ang 1-7 (16–22). Santos et al. (23) showed that Mas is expressed in the adipose tissue and that Mas-deficient mice develop a MetSyn-like state. In the current study, we evaluated the effect of long-term activation of the Mas receptor by chronic Ang 1-7 treatment on MetSyn in rats fed a high-fructose diet.

RESEARCH DESIGN AND METHODS

Animals and experimental design. Male Wistar rats (11–13 weeks old, 187 ± 1.3 g; Harlan, Rehovot, Israel) were housed in a light- and temperature-controlled room and were matched for weight in each experiment. All animals were handled according to the guidelines of the National Institutes of Health and the Weizmann Institute of Science for the management of laboratory animals.

Prevention experiment. Twenty-one rats served for this set of experiments, all of which were fed with high-fructose/low-magnesium diet (HFrD) (Research Diets, Inc., New Brunswick, NJ) for 26 weeks. Two weeks after the start of HFrD feeding, Alzet pumps filled with Ang 1-7 [Ang1-7 (DRVYIHP)] were implanted in six rats. Diet was composed of (in grams) fructose (610), casein (200), soybean oil (25), L-cystine (12), mineral mix (10), and vitamin mix (10). Magnesium concentration was 0.1% (compared with 1% in the normal chow diet). Low magnesium is known to disturb metabolic control and increase free radical–dependent oxidative tissue damage (24). Three male Wistar rats fed on normal chow served as one control group for the feeding regimen, and three male Wistar rats that were implanted with Alzet pumps filled with saline and fed on HFrD (HFrDSal) served as a control group for the pump implantation. Body weight was measured monthly, and a glucose tolerance test was carried out at the end of the 23rd week.

Short treatment experiment. Animals were assigned to two groups that were fed for 19 weeks with *1*) HFrD (n = 17) or *2*) normal standard chow (n = 13). After 19 weeks, Ang 1-7 pumps were implanted into nine HFrD rats and into seven of the normal chow rats. Ang 1-7 was administered via Alzet pumps [Ang1-7 (DRVYIHP)] for 1 month (short-term treatment). Body weight, fasting triglycerides (TGs), and glucose tolerance were assessed before and after treatment with Ang 1-7. In an additional treatment experiment, we studied the following groups: rats fed on regular chow (n = 3), HFrD rats (n = 8), and rats fed for 6 months on HFrD, followed by 2 months of Ang 1-7 treatment (n = 6).

Ang 1-7 was synthesized by the solid-phase methodology, using a multiple-peptide synthesizer AMS 422 (Abimed Analyzer Technik GmbH). An Alzet osmotic pump (2ML4; Strategic Applications Inc., Lake Villa, IL) was implanted subcutaneously, and Ang 1-7 (576 μg/kg rat/day in PBS) was delivered continuously at a constant rate for 4 weeks. This dose was chosen based on previous studies showing that Ang 1-7 administered chronically, via a mini-pump such as the one used by us, is clearly bioactive in the cardiovascular system, in which it has been studied extensively in recent decades (e.g., amelioration of diabetes-related cardiovascular dysfunction) (25). Insulin resistance was calculated by the homeostasis model assessment of insulin resistance (HOMA-IR) as follows: [fasting insulin (pmol/L) × fasting glucose (mmol/L)]/135 (26). Insulin levels were measured using an insulin radioimmunoassay kit (Diasorin Inc., Stillwater, MN). Glucose levels were measured by the Elite II glucometer (Bayer, Leverkusen, Germany). Serum aldosterone was measured by radioimmunoassay (Siemens, Los Angeles, CA).

Glucose tolerance test. After an overnight fast, samples (t = 0) were collected, and a solution of 50% glucose (2 g/kg body weight) was administered intraperitoneally. Blood was collected from the tail vein 30, 60, 90, and 120 min after glucose administration. All blood glucose measurements were performed using a hand-held glucometer (Elite II).

Insulin tolerance test. After a 6-h fast, baseline blood samples were obtained, followed by intraperitoneal injection of insulin (2 units/kg, Actrapid; Novo Nordisk) with blood sampling (from the tail) at 10, 20, 30, 40, 50, and 60 min.

Fat analysis by magnetic resonance imaging. Body fat was measured in six fructose-fed, Ang 1-7–treated rats and five fructose-fed rats by magnetic resonance imaging (MRI; 4.7 Tesla BioSpec Magnet 47/30 USR system; Bruker, Ettingen, Germany) equipped with a gradient coil system capable of producing a pulse gradient of up to 20 G/cm in each of the three dimensions. A detailed description of the MRI and means to calculate fat volume are provided in the Supplementary Data online.

Histological analysis. After 24 weeks of HFrD in the prevention experiment, rats were killed by sodium thiopental injection. Liver specimens and epididymal fat were fixed overnight in buffered formaldehyde (10%) and embedded in paraffin. Sections from the liver of each animal were stained with hematoxylin and eosin for evaluation of necro-inflammatory grading, oil red O for the evaluation of fatty droplets (macrovesicular or microvesicular steatosis), and masson trichrome for the evaluation of fibrosis. Histological changes were assessed by a modification of the scoring system for grading and staging for nonalcoholic steatohepatitis described by Brunt et al. (27). All slides were coded to keep the examiner blind to the experimental conditions during morphometric analysis. Five random visual fields (original magnification ×20) per each block (i.e., from each rat) from the liver were photographed, and an area including at least 150 adipocytes was analyzed using Image-Pro software (28).

Microscope and imaging. Images were acquired using a light Nikon E800 microscope (Nikon Instrument Group, Melville, NY) equipped with a Nikon DXM 1200 camera (Nikon Instrument Group). Measurements were performed using Image-Pro Plus 5.0 for Windows (Media Cybernetics, Bethesda, MD).

Immunohistochemical analyses of fat and liver tissues. Immunohistochemical analyses of fat and liver tissues were performed on adjacent paraffin sections using monoclonal antibodies against CD68 (a lysosomal membrane glycoprotein on macrophages). Antigen retrieval (epitomics) was performed by autoclaving in 0.01 M citrate buffer (pH 6.0) at 121°C for 10 min followed by 2 h incubation in blocking solution. Sections were reacted with a mouse monoclonal anti-CD68 primary antibody (1:200, MCA341GA; Serotec) overnight at 4°C according to a previously described method with minor modifications (28).

Tissue homogenization and Western blot analysis. Epididymal adipose tissue was homogenized with a Polytron in homogenization buffer (50 mM HEPES, pH 7.5, 0.5% NP-40, 1 mM EDTA, 1 mM EGTA, 150 mM NaCl, 1.5 mM $MgCl_2$, containing 1% protease inhibitor cocktail). The protein concentration was determined based on the Bradford assay. For nuclear extracts, tissues were homogenized on ice with a glass homogenizer using the buffer for nuclear extracts (50 mmol/L sodium phosphate buffer, pH 7.4, containing 1 mmol/L EDTA, 1% Triton X-100, 1 mmol/L 2-mercaptoethanol, 20 μg/mL leupeptin, and 1 μg/mL pepstatin). In brief, equal amounts of proteins were fractioned by SDS-PAGE, and proteins were then transferred to a nitrocellulose membrane (Protean nitrocellulose 85; Schleicher & Schuell, Dassel, Germany). Membranes were blocked with 20 mmol/L Tris, pH 7.6, 137 mmol/L NaCl, containing 0.1% Tween 20 and 2% BSA (TBST) for 60 min at room temperature, after which they were washed and incubated overnight at 4°C with the following antibodies: general extracellular signal–related kinase (ERK), p-ERK, glyceraldehyde-3-phosphate dehydrogenase (1:1,000; Sigma-Aldrich, St. Louis, MO), fatty acid synthetase (FAS), p-nuclear factor-κB (NFκB) p65 sc-33039, and MAS1 sc 54848 (1:1,000; Santa Cruz Biotechnology, Santa Cruz, CA). The membranes were subsequently washed and incubated for 1 h with peroxidase-labeled secondary antibody and processed for enhanced chemiluminescence (GE Healthcare, Danyel Biotech, Rehovot, Israel).

Measurement of O_2^- production. Equal weights of epididymal fat from HFrD rats (n = 4), HFrD Ang 1-7–treated rats (n = 4), and rats fed on normal chow (n = 3) were homogenized manually on ice with a glass homogenizer (Kontes, Vineland, NJ) by 10 strokes in 1 mL of homogenization buffer (20 mmol/L Tris-HCl, pH 7.4, 255 mM sucrose, 2 mmol/L EDTA, 2 mmol/L EGTA, 2 mmol/L dithiothreitol, 10 μg/mL leupeptin, and 0.1 mM phenylmethylsulfonyl fluoride). NADPH (100 μM) was added to 100 μL of lysate and incubated for 30 min at 37°C. O_2^- production was measured by addition of 5 μM lucigenin. The luminescence due to lucigenin was measured using VICTOR *X* multilabel plate readers (PerkinElmer, Waltham, MA). Arbitrary light counts were normalized using the Bradford protein assay.

Isolation and culture of extensor digitorum longus myofibers. Single muscle fibers were isolated from the extensor digitorum longus muscle as previously described (29).

Immunofluorescence. Primary antibodies were monoclonal and produced in mouse. Antibodies were diluted in the blocking solution (Tris-buffered saline,

TABLE 1
Effect of chronic Ang 1-7 infusion on metabolic parameters in the fructose-fed rat

	HFrD; n = 12	HFrD Ang 1-7; n = 6	HFrDSal pump; n = 3	Normal chow; n = 3
Body weight (g)	505 ± 12.52	457.16 ± 8.5[a]	538.75 ± 14.4	501.6 ± 13.54
Fasting glucose (mmol/L)	8.9 ± 0.4[b]	7.56 ± 0.2[a]	9.1 ± 0.69[b]	7 ± 0.15
Plasma insulin (pmol/L)	296.1 ± 20.8	234.9 ± 42.4	287 ± 34.5	189.8 ± 34
HOMA score	19.52 ± 0.06	13.15 ± 0.06[a]	19.35 ± 0.18[b]	9.84 ± 0.04
Triglycerides (mmol/L)	2.22 ± 0.24	1.09 ± 0.16[a]	2.9 ± 0.29	2.08 ± 0.14
Uric acid (μmol/L)	1.72 ± 0.11	1.62 ± 0.14	1.17 ± 0.14	1.9 ± 0.6
Creatinine (μmol/L)	0.61 ± 0.012	0.59 ± 0.006	0.59 ± 0.009	0.62 ± 0.01
Aldosterone (pmol/L)	543.22 ± 48.39	259.27 ± 32.59[a]	538.76 ± 215.75	437. 9 ± 35.18

[a]Significant difference ($P < 0.05$) between Ang 1-7–treated and untreated rats. [b]Significant difference ($P < 0.05$) between HFrD and normal chow rats.

1% goat serum). The following primary antibodies were used: anti-Pax7, mouse mAb [ascites fluid, 1:2,000 dilution; Developmental Studies Hybridoma Bank (DSHB)]; anti-MyoD, mouse mAb (IgG1, clone 5.8A, 1:800; BD Biosciences); and antisarcomeric myosin, mouse mAb (IgG2b, clone MF20, hybridoma supernatant, 1:20; DSHB).

Determination of the percent of myogenic cells out of total cells in myofiber cultures. Myogenic cells were detected in freshly isolated extensor digitorum longus myofiber cultures by coimmunolabeling with Pax7, which identifies proliferating myogenic cells, MyoD, which is a muscle-specific marker of proliferating and differentiating cells. Cultures were also immunostained with an antibody that recognizes skeletal muscle sarcomeric myosin, which identifies differentiating and fusing myogenic cells. The total number of nuclei present in the cultures was determined based on counting DAPI-positive nuclei. The percent of myogenic cells per culture was determined by calculating the relative number of myogenic cells out of total nuclei. Using a 20× objective, all cells within each culture were analyzed. Three images were acquired per field, using phase and fluorescent channels (red: Pax7, MyoD, and skeletal muscle sarcomeric myosin; blue: DAPI). Imaging was performed with an inverted fluorescent microscope (Axiovert 200M + AxiocamMRm monochrome CCD camera; Zeiss), controlled by AxioVision 4.4 Imaging System.

Statistics. Data are presented as mean ± SEM values calculated from at least six animals in each group. Results were analyzed using Student t test when data from two experimental groups were compared or ANOVA followed by post hoc Bonferroni multiple comparison test when data from three or more groups were studied. A nonparametric test was used when data did not distribute normally. $P < 0.05$ was considered statistically significant. The statistical analysis was performed using SPSS version 15 and STATISTICA version 9.

RESULTS

Metabolic characteristics of Ang 1-7–treated and untreated rats. After 6 months of feeding on HFrD with or without saline pumps, HFrDSal rats developed the MetSyn whereas rats fed on normal chow did not (Table 1). Ang 1-7–treated rats had significantly lower body weight than the HFrD and HFrDSal groups (457 ± 8.5, 505 ± 12.5, and 538.7 ± 14.4 g, respectively; $P < 0.05$) (Table 1). Remarkably, chronic treatment with Ang 1-7 significantly decreased fasting glucose and TG levels in comparison with the values measured in the HFrD and HFrDSal rats ($P < 0.05$). Additionally, HFrD Ang 1-7–treated rats had a significantly lower plasma renin concentration and serum aldosterone than the HFrD rats (94 ± 6.02 vs. 151 ± 9.2 ng/mL/h and 259.2 ± 32.5 vs. 543.2.7 ± 48.4 pmol/L, for renin and aldosterone, respectively; $P < 0.05$).

In the short-term (4 weeks) Ang 1-7 treatment experiment, there was no significant difference in weight gain between HFrD rats treated and untreated with Ang 1-7 (13 ± 3.3 vs. 17 ± 3.9 g, $P = 0.4$). When Ang 1-7 was administered chronically for 6 months, rats gained similar weight compared with rats fed on normal chow (143.6 ± 5.7 vs. 143.33 ± 8.7%, $P = 0.39$). Moreover, HFrD and

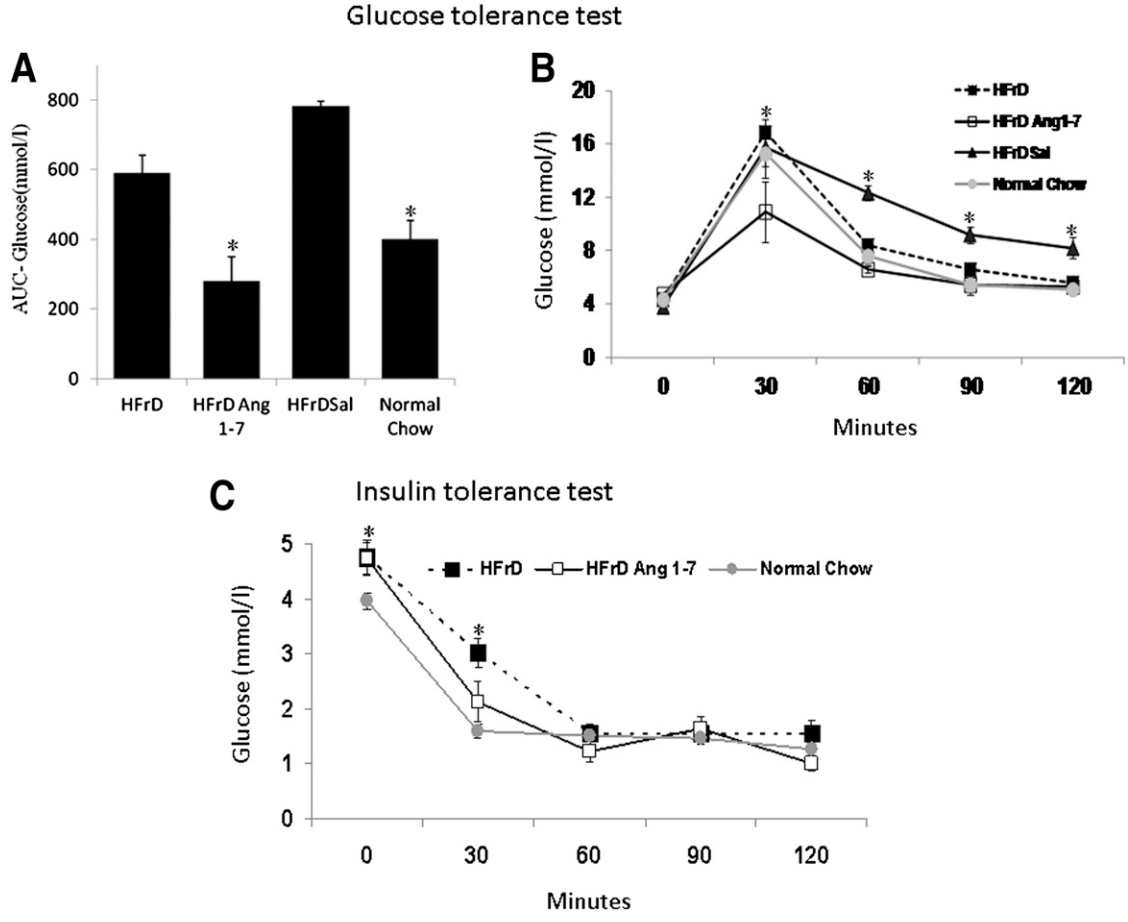

FIG. 1. Insulin sensitivity tests. *A* and *B*: Glucose tolerance test. Ang 1-7–treated rats ($n = 6$) had normal levels of basal serum glucose and insulin but a significantly attenuated increase in serum glucose response to acute (2 g/kg) intraperitoneal glucose challenge, compared with fructose-fed rats ($n = 9$, $P < 0.05$), as revealed by the AUC analysis (*A*). Glucose levels were measured 30, 60, and 90 min after injection and were significantly reduced by Ang 1-7 at 30, 60, and 90 min postinjection ($P < 0.05$) (*B*). Data are presented as the mean value ± SEM. *C*: Intraperitoneal insulin tolerance test. Ang 1-7 rats had increased insulin sensitivity with a more prominent and prolonged hypoglycemic effect of insulin. Changes in basal ($t = 0$) blood glucose levels after intraperitoneal insulin administration were measured every 30 min over a total period of 120 min. Ang 1-7 treatment led to a significant hypoglycemic reaction at 30 and 120 min post–insulin reduction ($P < 0.05$). Data are presented as the mean value ± SEM. *$P < 0.05$.

HFrDSal groups showed a weight gain of 159.8 ± 4.98 and 150.22 ± 4.75%, respectively.

Serum TG levels were markedly higher in the HFrD compared with normal chow rats (3.11 ± 0.45 vs. 0.98 ± 0.05 mmol/L, $P < 0.05$). No change in serum TGs was noted in rats that were fed with normal chow and treated with Ang 1-7. There was a marked reduction of serum TGs, insulin levels, and HOMA-IR in rats that were fed on HFrD and treated with Ang 1-7 for 1 month (3.11 ± 0.45 vs. 2.43 ± 0.32 mmol/L, $P < 0.05$, 184 ± 13.9 vs. 120 ± 16 pmol/L, $P < 0.05$, and 5.26 ± 0.08 vs. 3.4 ± 0.08, $P < 0.05$, respectively) (Supplementary Appendix).

Chronic treatment with Ang 1-7 improves insulin sensitivity of HFrD rats. The response to an intraperitoneal glucose tolerance test (IPGTT) after 6 months of Ang 1-7 treatment is shown in Fig. 1. Compared with the HFrD group, the Ang 1-7–treated group presented a significantly smaller rise in glucose, as reflected in the area under the curve (AUC) of glucose levels during the IPGTT (589.3 ± 51.6 vs. 279.3 ± 71.2 mmol/L, respectively, $P < 0.001$) (Fig. 1*A*). Differences in glucose levels were prominent at 30, 60, and 90 min after the injection (10.9 ± 2.2 vs. 16.85 ± 1.01, 6.6 ± 0.2 vs. 8. 39 ± 0.48, and 5.4 ± 0.3 vs. 6.6 ± 0. 25 mmol/L, respectively; $P < 0.05$) (Fig. 1*B*).

In the short treatment arm, there was no difference in glucose levels during IPGTT between the control and the Ang 1-7–treated rats ($P = 0.55$). However, glucose levels during the IPGTT were significantly lower in HFrD rats that were treated with Ang 1-7 compared with the untreated rats ($P < 0.05$) (see AUC in Supplementary Table 1).

Insulin sensitivity was further tested by means of the insulin tolerance test. After a 6-h fast, the chronic HFrD/Ang 1-7–treated and normal chow groups had lower glucose levels compared with the HFrD rats 30 and 120 min after insulin (2 units/kg rat) administration (2.13 ± 0.2 and 1.59 ± vs. 3 ± 0.3 and 1 ± 0.1 and 1.28 ± 0.130 vs. 1.55 ± 0.2 mmol/L, respectively; two-way ANOVA, $F_{(2,74)} = 6.5146$, $P = 0.05$) (Fig. 1*C*). Additionally, hypoglycemia developed earlier and recovery from hypoglycemia was delayed in the Ang 1-7–treated group. The AUC analysis did not reveal any difference, however (as can be inferred from Fig. 1*C*).

Fat analysis by MRI. Chronic treatment with Ang 1-7 decreased total body fat and subcutaneous fat: 29.593 ±

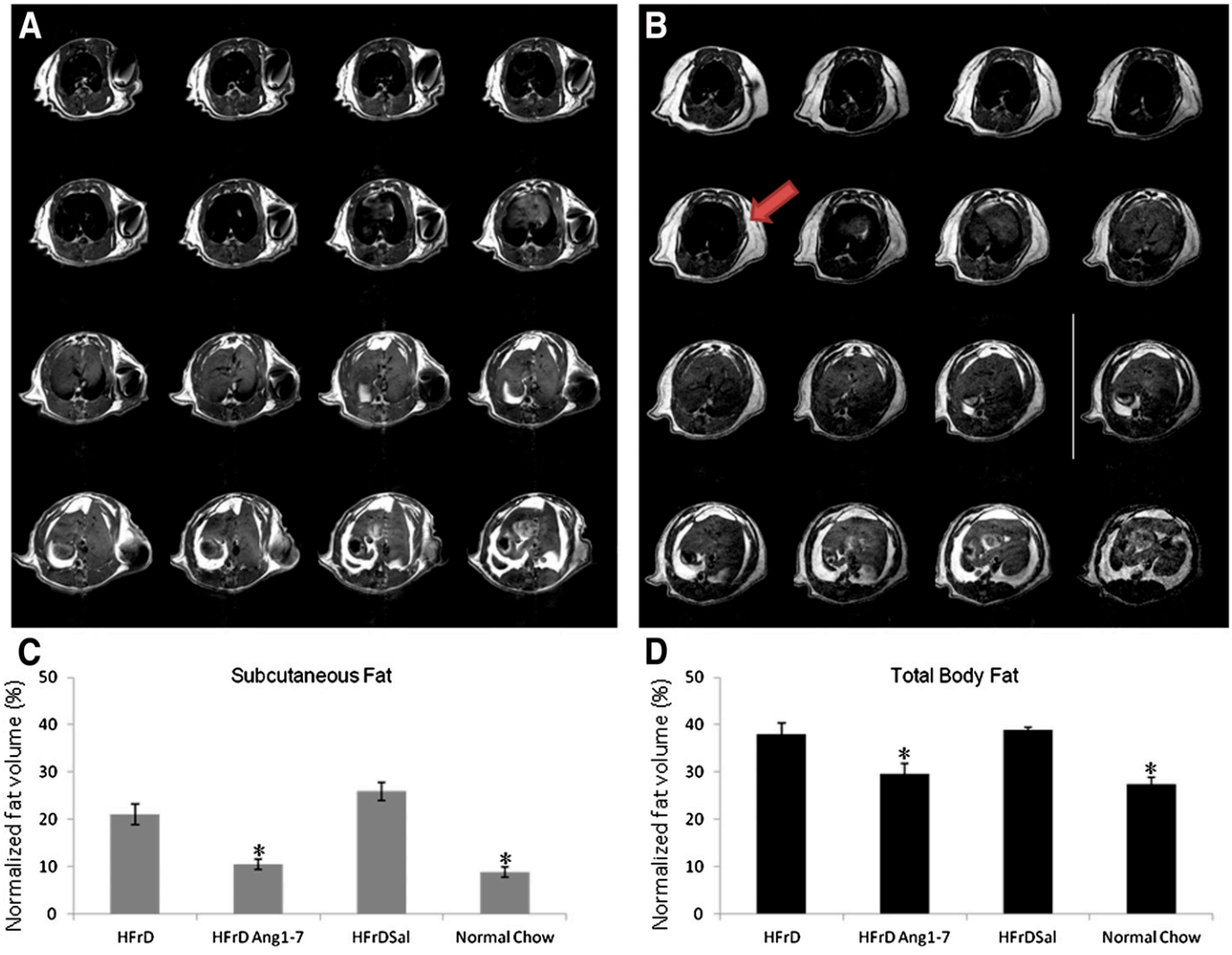

FIG. 2. MRI analysis of total and subcutaneous fat. Total and subcutaneous (red arrow pointing to subcutaneous fat) fat was significantly reduced in the 6-month HFrD Ang 1-7–treated rats ($n = 6$) (*A*) compared with HFrD-untreated rats ($n = 5$) (*B*). Averages ± SEM of total and subcutaneous fat in all studied groups are presented in *C* and *D*. *$P < 0.05$. (A high-quality color representation of this figure is available in the online issue.)

2.349 vs. 38.054 ± 2.161 cm^3 ($P < 0.05$) and 23.056 ± 2.183 vs. 10.432 ± 1.097 cm^3 ($P < 0.05$), respectively. Visceral fat was not measured (Fig. 2).

Adipocyte size and inflammation. Epididymal adipocytes in the Ang 1-7–treated animals were markedly smaller than those of the two control groups (mean adipocyte area: 4,133 ± 326 vs. 7,962 ± 1,161 and 8,687.925 ± 75.74 μm^2, $P = 0.008$) (Fig. 3*A* and *B*). Significantly less macrophages ($CD68^+$ cells) were detected in the epididymal fat of Ang 1-7–treated rats, suggesting lesser inflammation (5 ± 2 vs. 63 ± 35 $CD68^+$ cells per 20× field, $P < 0.05$) (Fig. 3*C*–*F*).

Grading and staging of degree of fatty liver infiltration. Ang 1-7–treated rats had diminished fat accumulation in the liver ($P < 0.05$), reduced lobular inflammation ($P < 0.05$), and less fibrosis ($P < 0.05$). No significant change was noted in portal inflammation (Fig. 4).

Treatment of HFrD rats with Ang 1-7 is associated with decreased phosphorylation of P65NFκB and ERK in epididymal fat. Since the ERK and NFκB pathway are key molecules in antioxidative/anti-inflammatory pathways, we examined the abundance of these molecules in the nuclei of adipocytes (from epididymal adipose tissue) of Ang 1-7–treated rats. Chronic treatment with Ang 1-7 resulted in decreased phosphorylation of P65NFκB (21 ± 1.43 vs. 53 ± 9.8 units, $P = 0.03$) (Fig. 5*C*) and ERK (68.8 ± 3.4 vs. 81.6 ± 2.3 units, $P = 0.01$) (Fig. 5*D*).

Ang 1-7 upregulates FAS expression in adipose tissue. FAS is involved in adipocyte lipid accumulation by regulating de novo lipogenesis from acetyl-CoA, malonyl-CoA, and NADPH. FAS is expressed at high levels in adipose tissue, liver, and lung. Treatment with thiazolidinedione, which ameliorates insulin resistance, is known to upregulate the adipocyte lipid storage genes diacylglycerol transferase and *FAS* (30). By upregulating these genes, adipocytes efficiently store lipids and prevent ectopic lipid deposition. A sucrose-rich diet is known to decrease FAS activity in adipose tissue (30). As shown in Fig. 5*B*, 6 months of Ang 1-7 treatment induced the upregulation of FAS expression in epididymal fat (31 ± 2.9 vs. 20.3 ± 1.3, arbitrary density units, $P = 0.01$) (Fig. 5*C*).

Mas receptor is expressed in adipose tissue and chronic Ang 1-7 treatment further upregulates its expression. Mas protein was detected in epididymal fat by Western blot analyses. Further, chronic treatment with Ang 1-7 for 6 months upregulated Mas expression in HFrD rats (55 ± 2 vs. 43.8 ± 2.8, arbitrary density units, $P = 0.01$) (Fig. 5*A*).

Effect of Ang 1-7 treatment on O_2^- production in epididymal fat. Fructose-fed rats have increased expression and activation of aortic NADPH oxidase, increased ventricular and vascular superoxide anion production (31), and elevated levels of free radical hydrogen peroxide (32). As blockade of Ang II receptor ameliorates adipocytokine dysregulation partly by decreasing oxidative stress in adipose tissue (33), we postulated that treatment with Ang 1-7 may have a similar effect. The lucigenin-enhanced chemiluminescence method was used to quantify the production levels of superoxide upon NADPH stimulation. Our results show that in epididymal fat homogenates, NADPH stimulated superoxide production, and that this stimulation was significantly lower in HFrD Ang 1-7–treated rats (42 ± 8%) than in untreated HFrD rats (165 ± 47% of control rats, $P < 0.04$) (Fig. 6).

Effect of Ang 1-7 treatment on skeletal muscle tissue ex vivo. To evaluate the effect of continuous infusion of Ang 1-7 on skeletal muscles, we cultured single myofibers for 10 days and determined the percent of myogenic cells

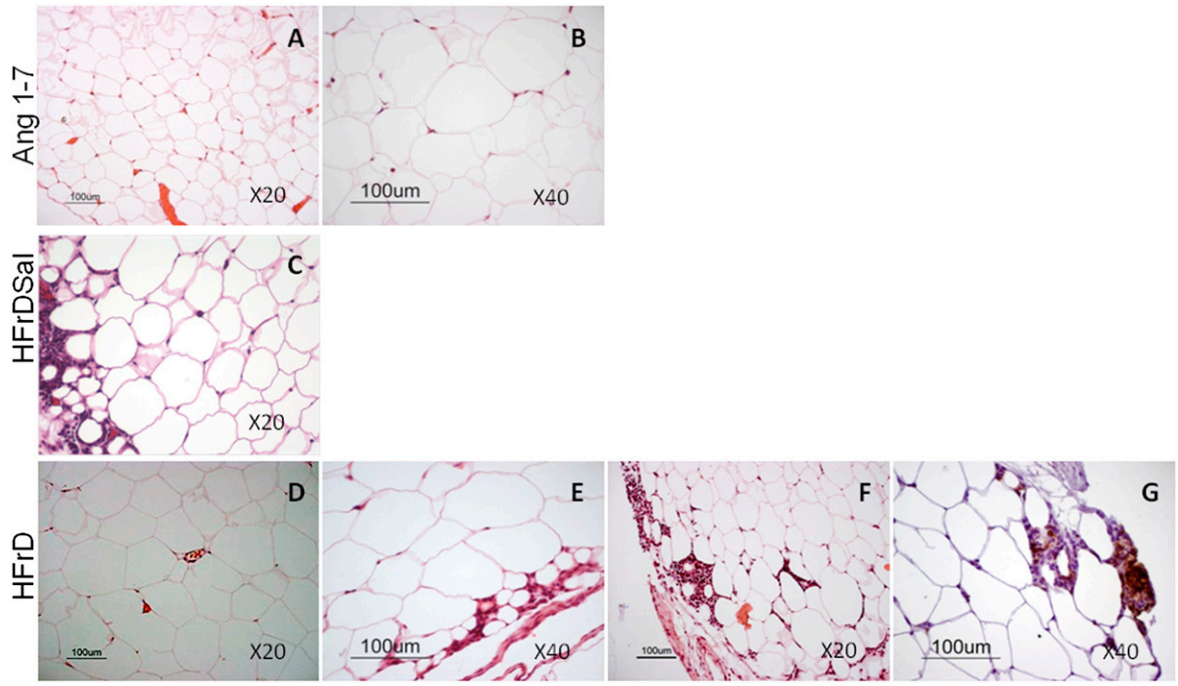

FIG. 3. Histological sections of epididymal fat tissue. Tissue sections from Ang 1-7–treated rats ($n = 6$) (*A* and *B*) display many small adipocytes and fewer large adipocytes (a field "enriched" with large adipocytes is shown in *B*). The large adipocytes did not display inflammatory infiltration. Tissue from HFrD and HFrDSal rats ($n = 9$) (*C*–*G*) displays large adipocytes with inflammatory infiltration (*C*, *E*, and *F*), mostly of macrophages (CD68 staining) (*G*). um, μm.

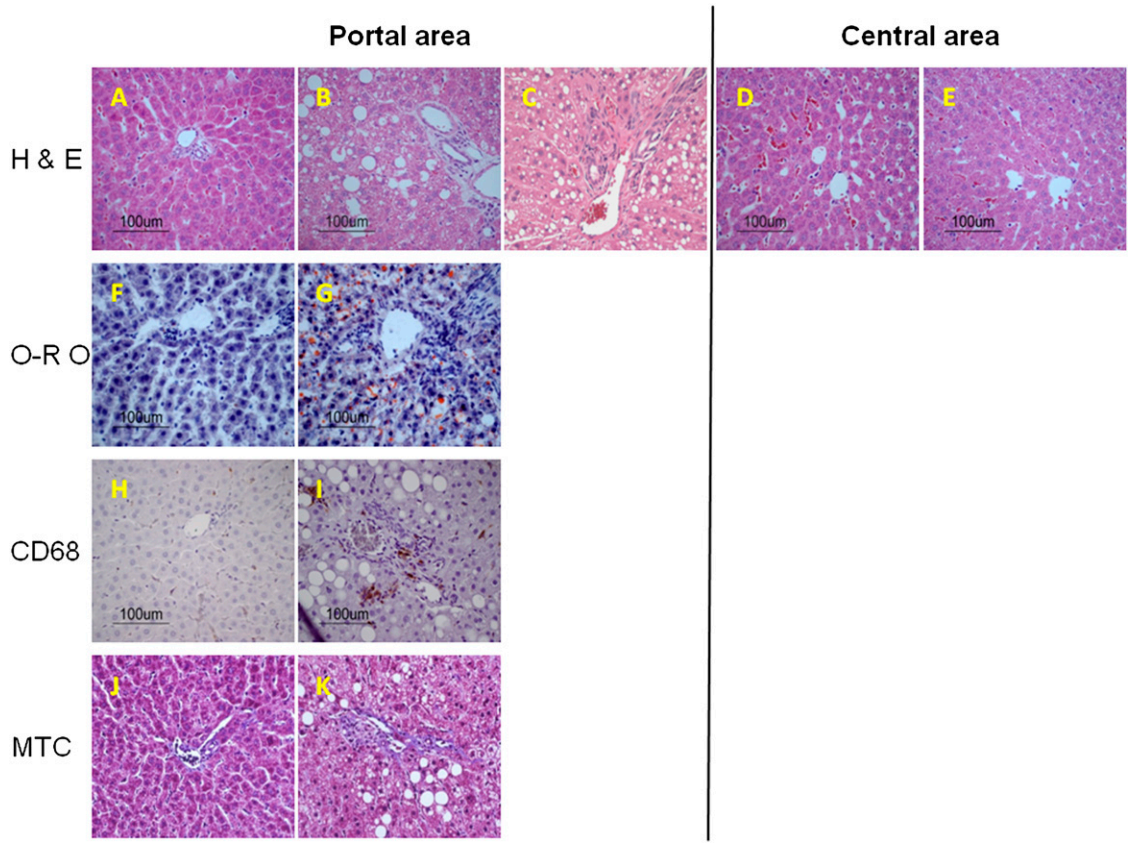

FIG. 4. Histological sections of the liver from animals in the prevention arm. Photomicrographs of portal (*A–C*) and central (*D* and *E*) regions of liver samples stained with hematoxylin and eosin (H & E). Portal areas of livers from HFrD Ang 1-7–treated rats ($n = 6$) (*A*, *F*, *H*, and *J*) and HFrDSal (*C*) and HFrD rats ($n = 9$) (*B*, *G*, *I*, and *K*) stained with oil red O (O-R O) (*F* and *G*), CD68 (*H* and *I*), and masson trichrome (MTC) (*J* and *K*). Original magnification ×40. Scale bar, 100 μm.

out of total cells. Myofibers isolated from fructose-fed, Ang 1-7–treated rats gave rise to cultures that contained ~80% myogenic cells and ~20% nonmyogenic cells, whereas cultures that developed from myofibers isolated from fructose only–treated rats were composed mostly of nonmyogenic cells. Fully differentiated adipocytes were present in most cultures that developed from myofibers from control rats. No adipocytes were detected in cultures from Ang 1-7–treated rats (Fig. 7). This suggests that the balance between myogenic and nonmyogenic cells is adversely affected under insulin-resistant conditions and that Ang 1-7 is involved in tipping the scale toward myogenesis.

Metabolic effects of Ang 1-7 treatment of rats with established MetSyn. In addition to establishing the combined long-term effects of Ang 1-7 and HFrD, we examined the influence of 2 months (i.e., short term) of Ang 1-7 treatment in rats already afflicted with the dysmetabolic effects of long-term consumption of HFrD. The working hypothesis was that Ang 1-7 not only prevents but also is able to mend the metabolic disturbances seen with the MetSyn.

For this, we studied the following groups: rats fed on regular chow ($n = 3$), HFrD rats ($n = 8$), and rats fed for 6 months on HFrD followed by 2 months of Ang 1-7 treatment ($n = 6$).

By the end of this 2-month intervention, we found that HFrD Ang 1-7–treated rats weighed less than the HFrD-untreated rats (HFrD, 543 ± 27.2 g; HFrD + Ang 1-7, 518.3 ± 17.5 g; normal chow, 501 ± 16.5 g; $P < 0.05$; baseline weights of the HFrD groups were not different), had lower total body fat mass (HFrD, 43.3 ± 0.7 cm^3; HFrD + Ang 1-7, 39.6 ± 1.25 cm^3; normal chow, 27.36 ± 1.6 cm^3; $P < 0.05$), had lower visceral fat mass (HFrD, 28.5 ± 0.7 cm^3; HFrD + Ang 1-7, 24.7 ± 1.5 cm^3; normal chow, 18.5 ± 0.66 cm^3; $P < 0.05$), and had lower serum TGs (HFrD, 266.3 ± 30 mg/dL; HFrD + Ang 1-7, 173.5 ± 25.5 mg/dL; normal chow, 104.6 ± 5 mg/dL; $P < 0.05$). Of note is the finding that in parallel to the effect of long-term Ang 1-7 treatment, just 2 months of Ang 1-7 treatment administered at a late phase of exposure to high fructose intake was sufficient to induce reduction in the mean size of epididymal fat cells (HFrD, 5,990 ± 721 μm^2; HFrD + Ang 1-7, 3,862 ± 599 μm^2; normal chow, 3,671 ± 767 μm^2; $P < 0.05$).

Using an insulin challenge dose of 0.8 units/kg of regular insulin (injected after a 6-h fast), 2 months of treatment with Ang 1-7 clearly increased the sensitivity to insulin. As compared with the HFrD-only and normal chow rats, glucose levels were lower in the HFrD rats treated with Ang 1-7, as measured 50 and 60 min after the intraperitoneal insulin injection (42.1 ± 2.3 vs. 55 ± 1.92 and 51.6 ± 4.97 mg/dL, respectively, at 50 min; two-way ANOVA, $F_{(2, 105)} = 4.1404$, $P < 0.05$). The postinsulin glucose nadir value was also the lowest and most prolonged in the Ang 1-7–treated group (39.2 ± 2.6 vs. 49.25 ± 2.07 and 51.6 ± 4.46 mg/dL at 60 min postinsulin injection, respectively, $P < 0.05$).

DISCUSSION

In this study, we show that in fructose-fed rats, chronic treatment with Ang 1-7 resulted in multiorgan protection from the effects of the MetSyn, including reduction in

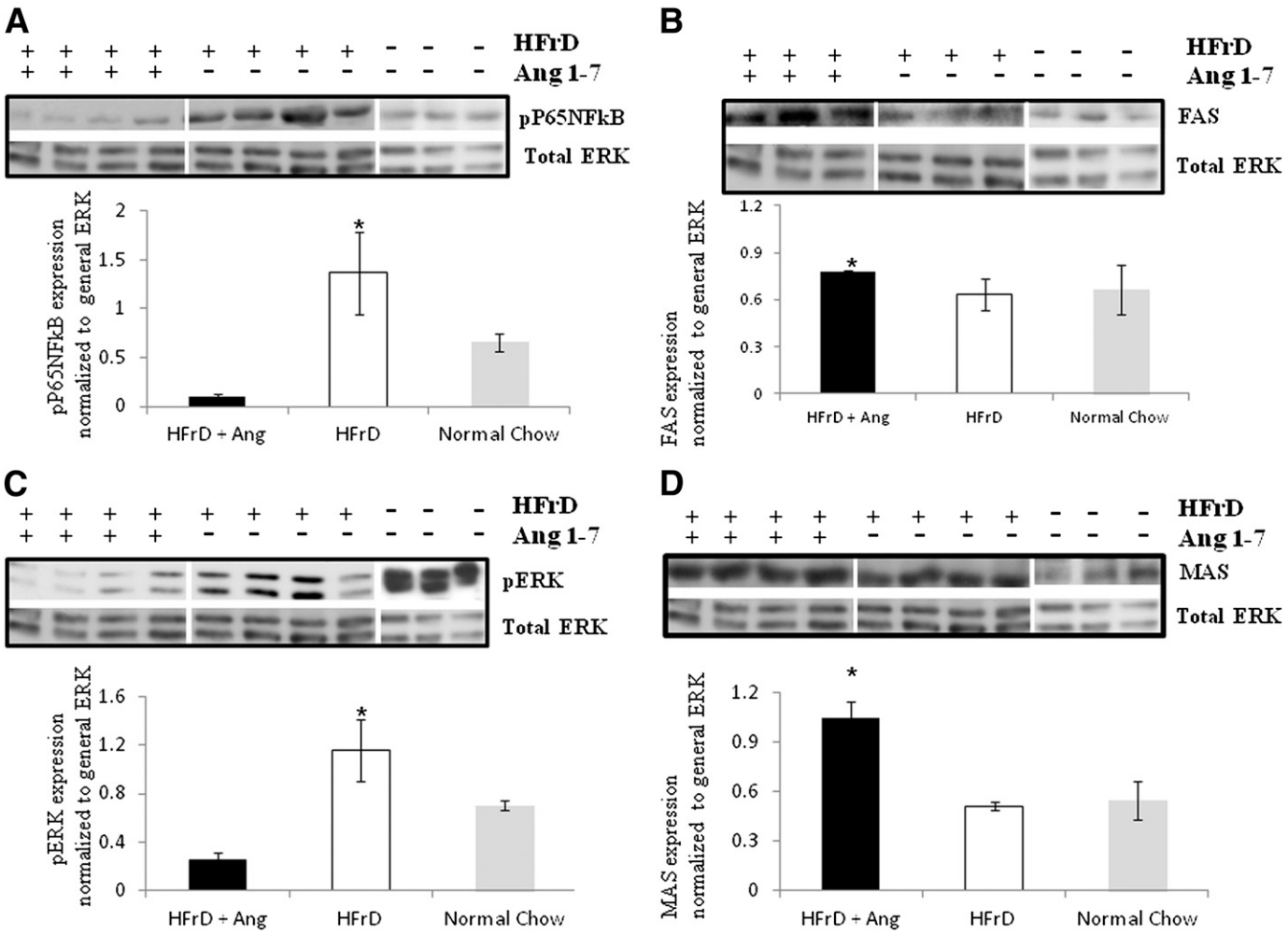

FIG. 5. Expression of pP65NFκB, FAS, MAS, and activated ERK in the epididymal fat of rats treated with Ang 1-7 for 6 months (n = 6) and control rats (n = 9). Ang 1-7 treatment significantly reduced the levels of phosphorylated p65 (*A*) and of phosphorylated ERK (*C*). Elevated levels of FAS were evident in the Ang 1-7–treated group (*B*); however, no downregulation of the Ang 1-7 receptor, MAS, was detected (*D*). Bar graphs represent a quantification of the respective protein expression levels from at least three experiments. Data are presented as mean ± SEM. *P < 0.05.

weight gain, insulin resistance, TGs and aldosterone levels, adipositis, and hepatosteatitis. Additionally, in vivo Ang 1-7 treatment *1*) improved the myogeneity of primary skeletal muscle fiber cultures compared with cultures from untreated fructose-fed rats and *2*) eliminated the formation of adipocytes in this setting. Of critical significance is the finding that 4 weeks of Ang 1-7 treatment of fructose-fed rats was associated with improvement in glucose sensitivity and fasting hypertriglyceridemia without any changes in body weight. Hence, Ang 1-7 can affect glucose and fat trafficking in vivo prior to, and therefore independent of, changes in body weight. Still, a role for the somewhat lower weight (~9.5%) attained by very long Ang 1-7 treatment in fructose-fed rats in some of the long-term findings in this study cannot be entirely excluded. Our data show an improvement in insulin resistance upon Ang 1-7 treatment, suggesting that Ang 1-7 could have a potential role in the treatment of the MetSyn. This is in concert with recent papers of Santos et al. (23,34) and Giani et al. (35), showing the evolution of the MetSyn-like state with Mas deficiency and improved insulin resistance with Ang 1-7 treatment.

We used an experimental model in which insulin resistance evolves spontaneously (36). The uniqueness of this model is that it features many similarities with the development of insulin resistance in humans that feed on a high-carbohydrate diet. Under these conditions, insulin resistance is acquired as a result of activation of the sympathetic nervous system, increased production of vasoconstrictors such as endothelin-1, Ang II, and prostanoids in conjunction with increased oxidative stress (37). Additionally, choosing this specific type of diet was based on its similarity to the Western diet in that the consumption of fructose significantly increased and that of magnesium decreased. Moreover, elevated fructose and lower magnesium were suggested to have direct causal deleterious effects in the epidemics of obesity and type 2 diabetes both in pediatric and adult populations (38). In the choice to enrich the diet with fructose up to 60% [compared with 10% described in the article of Giani et al. (35)], we aimed to study the effects of Ang 1-7 on a more severe state of chronic dyslipidemia and hyperglycemia.

Shinozaki et al. (39) reported that in fructose-fed rats, insulin resistance is associated with upregulation of the AT1a receptor and increased endothelial O_2^- production caused by activation of NADPH oxidase. Furthermore, blockade of the AT1 receptor reversed these effects (32). Here we found elevated superoxide production in the rat's

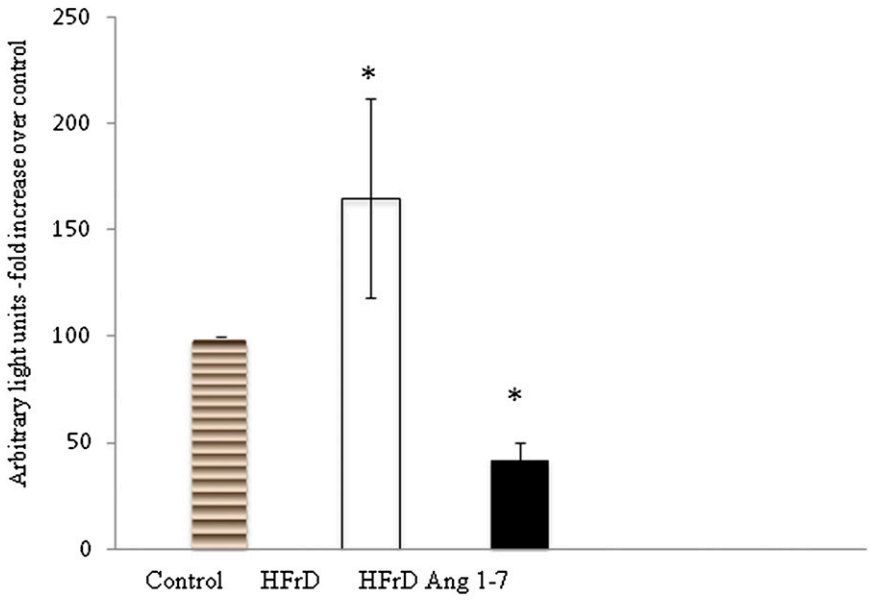

FIG. 6. Epididymal fat NADPH-stimulated superoxide production as measured by lucigenin-enhanced chemiluminescence. Superoxide production was significantly lower in HFrD rats treated with Ang 1-7 compared with HFrD-untreated rats [fructose untreated (n = 5), 165 ± 47% of control rats; fructose + Ang 1-7 (n = 5), 42 ± 8% of control rats (n = 3); P < 0.05 in comparison with control values]. Data are presented as the mean ± SE. *P < 0.05. (A high-quality color representation of this figure is available in the online issue.)

epididymal fat, which was countered by Ang 1-7 treatment. Moreover, Ang 1-7 also reduced the activation of NFκB and ERK in adipose tissue, which accords with the decrease in adipose tissue macrophages and improved fat cell size and function (as implied by increased FAS expression).

Increased fat accumulation in the liver is a marker of hepatic insulin resistance and a close correlate of all components of the MetSyn, independent of obesity (40). Fatty liver is also an independent predictor of the MetSyn, type 2 diabetes, and cardiovascular disease (41). Adipose tissue inflammation and a fatty liver seem to coexist, but

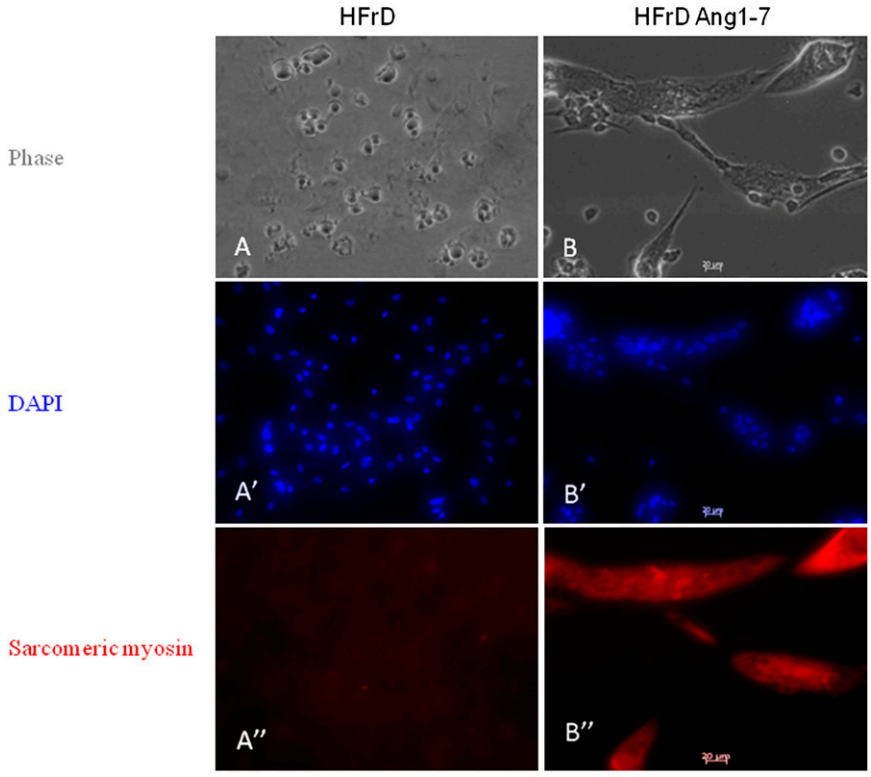

FIG. 7. Immunofluorescence of 10-day myofiber cultures. Individual myofibers were isolated from HFrD rats that were not (A, A', and A'') or were treated with Ang 1-7 (B, B', and B''). At least nine cultures per rat (three HFrD and four HFrD Ang 1-7 rats) were reacted with DAPI to allow visualization of nuclei (A' and B') and sarcomeric myosin for specific identification of skeletal muscle cells (A'' and B''). Scale bar, 20 μm.

the direction of causality, if any, is unclear. In mice, overexpression of CCL2 (MCP1) in adipose tissue leads to macrophage accumulation and steatosis (42), whereas CCR2 (CCL2 receptor) deficiency reduces adipose tissue macrophage content, increases adiponectin expression, and ameliorates hepatic steatosis (43). On the other hand, hepatic activation of NFκB in mice via overexpression of IκB kinase β induces insulin resistance in the liver and signs of systemic inflammation (increase in serum IL-6) and insulin resistance in skeletal muscle (44).

We found adipositis and steatohepatitis in the HFrD group, but rats treated with Ang 1-7 showed reduced hepatic fat accumulation, lobular inflammation, and fibrosis. This is concordant with observations that the Ang 1-7 antagonist (A-779) aggravates hepatic fibrosis in a model of bile duct ligation (45). Here we noticed that liver fibrosis induced simply by dietary means (i.e., high fructose), which corresponds better with nonalcoholic liver disease in humans (46), could be prevented by Ang 1-7.

Aldosterone may have a role in the pathogenesis of the MetSyn. The prevalence of the MetSyn is higher in patients with primary hyperaldosteronism than in essential hypertension (47). Moreover, aldosterone, through nongenomic actions, can interfere with intracellular insulin signaling and lead to impaired glucose homeostasis and systemic insulin resistance in skeletal muscle, liver, and cardiovascular tissue (48). The significant reduction in aldosterone levels upon prolonged Ang 1-7 treatment was concordant with parallel effects on circulating plasma renin activity. However, additional interactions cannot be excluded, such as a direct adrenal effect of Ang 1-7 or indirect effects through renin or aldosterone-releasing factor, which is released from adipocytes in response to oxidative stress load. This reduction in aldosterone may have contributed to some of the beneficial effects of Ang 1-7, particularly the reduction in liver fibrosis and NADPH oxidase activity.

This is the first report that Ang 1-7 treatment in vivo can modify the myofiber culture phenotype as studied ex vivo. Whereas myofibers derived from Ang 1-7–treated rats gave rise to cultures that contained 80% myogenic cells and were entirely devoid of fully developed adipocytes, myofiber cultures from the HFrD control rats were composed mostly (i.e., 60%) of nonmyogenic cells, including fully differentiated fat cells. This finding is of interest in light of the direct correlation between the enhanced content of intermuscular adipocytes and insulin resistance (9). The development of nonmyogenic cells (such as adipocytes or fibroblasts) in addition to myoblasts in cultures emanating from myofibers has put forth the hypothesis that satellite cells may possess mesenchymal plasticity and can thus embark on a nonmyogenic differentiation path. Alternatively, such nonmyogenic cells may be the progeny of mesenchymal stem cells present in the muscle that were co-isolated with the myofiber. Regardless of their origin, augmentation of nonmyogenic cells instead of muscle cells may impede proper muscle function and repair. Because sarcopenia is a major obstacle in aging and diabetes (8), the possibility that Ang 1-7 may somehow participate in satellite cell commitment to take on a preferentially myogenic route is of much potential interest and deserves further elucidation.

Further studies are needed to scrutinize the effects of Ang 1-7 in the MetSyn. The beneficial effects we report here may be related to the direct anti-inflammatory and antioxidative effects of Ang 1-7 or to opposing Ang II effects (i.e., indirect effects). Recently, Ang II was shown to decrease ligand-mediated peroxisome proliferator–activated receptor γ transcriptional activity through increased Bcr expression and kinase activity (49), whereas Ang 1-7 may increase peroxisome proliferator–activated receptor γ expression (50). Thus, new potential metabolic interactions between Ang II and Ang 1-7 must be explored in the context of the MetSyn.

In all, our results demonstrate that chronic treatment with Ang 1-7 had an ameliorating effect on insulin resistance, hypertriglyceridemia, fatty liver, obesity, and adipositis in the HFrD rats. Further, the balance between myogenic and nonmyogenic (including adipogenic) cells in skeletal muscle is impaired in this model of the MetSyn, but can be favorably affected by long-term Ang 1-7 administration. These results comprise the first evidence that Ang 1-7 can provide multisystem protection from the metabolic sequels of exposure to high fructose.

ACKNOWLEDGMENTS

No potential conflicts of interest relevant to this article were reported.

Y.M. designed, conducted, and analyzed experiments and wrote the manuscript. G.S. conducted and analyzed some of the experiments and wrote the manuscript. K.S., R.L., and N.N. conducted some of the experiments. F.K. conducted some of the experiments and contributed to discussion. O.P. analyzed some of the experiments. I.B. performed the MRI scan and provided MRI raw data. M.B. helped perform some of the experiments. T.B. cut sections and performed histochemical stainings. M.F. contributed to discussion. D.B. and Y.S. edited the manuscript. N.S. contributed to discussion and wrote, reviewed, and edited the manuscript. N.S. is the guarantor of this work and, as such, had full access to all the data in the study and takes responsibility for the integrity of the data and the accuracy of the data analysis.

The authors are grateful for the expert assistance of Prof. Rony Zeger and Tamar Hanoch (Department of Biological Regulation, Weizmann Institute of Science) in the study of protein expression of the fat tissue extracts.

REFERENCES

1. Bays H, Rodbard HW, Schorr AB, González-Campoy JM. Adiposopathy: treating pathogenic adipose tissue to reduce cardiovascular disease risk. Curr Treat Options Cardiovasc Med 2007;9:259–271
2. Matsuzawa Y. The metabolic syndrome and adipocytokines. FEBS Lett 2006;580:2917–2921
3. Holt HB, Wild SH, Wood PJ, et al. Non-esterified fatty acid concentrations are independently associated with hepatic steatosis in obese subjects. Diabetologia 2006;49:141–148
4. Abuissa H, Jones PG, Marso SP, O'Keefe JH Jr. Angiotensin-converting enzyme inhibitors or angiotensin receptor blockers for prevention of type 2 diabetes: a meta-analysis of randomized clinical trials. J Am Coll Cardiol 2005;46:821–826
5. Bataller R, Sancho-Bru P, Ginès P, Brenner DA. Liver fibrogenesis: a new role for the renin-angiotensin system. Antioxid Redox Signal 2005;7:1346–1355
6. Stump CS, Henriksen EJ, Wei Y, Sowers JR. The metabolic syndrome: role of skeletal muscle metabolism. Ann Med 2006;38:389–402
7. Wei Y, Sowers JR, Nistala R, et al. Angiotensin II-induced NADPH oxidase activation impairs insulin signaling in skeletal muscle cells. J Biol Chem 2006;281:35137–35146
8. Pedersen M, Bruunsgaard H, Weis N, et al. Circulating levels of TNF-alpha and IL-6-relation to truncal fat mass and muscle mass in healthy elderly individuals and in patients with type-2 diabetes. Mech Ageing Dev 2003;124:495–502
9. Greco AV, Mingrone G, Giancaterini A, et al. Insulin resistance in morbid obesity: reversal with intramyocellular fat depletion. Diabetes 2002;51:144–151

10. Scarda A, Franzin C, Milan G, et al. Increased adipogenic conversion of muscle satellite cells in obese Zucker rats. Int J Obes (Lond) 2010;34:1319–1327
11. Durschlag RP, Layman DK. Skeletal muscle growth in lean and obese Zucker rats. Growth 1983;47:282–291
12. Santos RA, Ferreira AJ, Pinheiro SV, Sampaio WO, Touyz R, Campagnole-Santos MJ. Angiotensin-(1-7) and its receptor as a potential targets for new cardiovascular drugs. Expert Opin Investig Drugs 2005;14:1019–1031
13. Trask AJ, Ferrario CM. Angiotensin-(1-7): pharmacology and new perspectives in cardiovascular treatments. Cardiovasc Drug Rev 2007;25:162–174
14. Ferreira AJ, Santos RA. Cardiovascular actions of angiotensin-(1-7). Braz J Med Biol Res 2005;38:499–507
15. Raizada MK, Ferreira AJ. ACE2: a new target for cardiovascular disease therapeutics. J Cardiovasc Pharmacol 2007;50:112–119
16. Santos RA, Campagnole-Santos MJ, Andrade SP. Angiotensin-(1-7): an update. Regul Pept 2000;91:45–62
17. Schmaier AH. The kallikrein-kinin and the renin-angiotensin systems have a multilayered interaction. Am J Physiol Regul Integr Comp Physiol 2003;285:R1–R13
18. Carey RM, Siragy HM. Newly recognized components of the renin-angiotensin system: potential roles in cardiovascular and renal regulation. Endocr Rev 2003;24:261–271
19. Burrell LM, Johnston CI, Tikellis C, Cooper ME. ACE2, a new regulator of the renin-angiotensin system. Trends Endocrinol Metab 2004;15:166–169
20. Ferrario CM. Does angiotensin-(1-7) contribute to cardiac adaptation and preservation of endothelial function in heart failure? Circulation 2002;105:1523–1525
21. Campbell DJ. The renin-angiotensin and the kallikrein-kinin systems. Int J Biochem Cell Biol 2003;35:784–791
22. Roks AJ, van Geel PP, Pinto YM, et al. Angiotensin-(1-7) is a modulator of the human renin-angiotensin system. Hypertension 1999;34:296–301
23. Santos SH, Fernandes LR, Mario EG, et al. Mas deficiency in FVB/N mice produces marked changes in lipid and glycemic metabolism. Diabetes 2008;57:340–347
24. Olatunji LA, Soladoye AO. Increased magnesium intake prevents hyperlipidemia and insulin resistance and reduces lipid peroxidation in fructose-fed rats. Pathophysiology 2007;14:11–15
25. Benter IF, Yousif MH, Cojocel C, Al-Maghrebi M, Diz DI. Angiotensin-(1-7) prevents diabetes-induced cardiovascular dysfunction. Am J Physiol Heart Circ Physiol 2007;292:H666–H672
26. Nagaretani H, Nakamura T, Funahashi T, et al. Visceral fat is a major contributor for multiple risk factor clustering in Japanese men with impaired glucose tolerance. Diabetes Care 2001;24:2127–2133
27. Brunt EM, Janney CG, Di Bisceglie AM, Neuschwander-Tetri BA, Bacon BR. Nonalcoholic steatohepatitis: a proposal for grading and staging the histological lesions. Am J Gastroenterol 1999;94:2467–2474
28. Kudo H, Yata Y, Takahara T, et al. Telmisartan attenuates progression of steatohepatitis in mice: role of hepatic macrophage infiltration and effects on adipose tissue. Liver Int 2009;29:988–996
29. Shefer G, Carmeli E, Rauner G, Yablonka-Reuveni Z, Benayahu D. Exercise running and tetracycline as means to enhance skeletal muscle stem cell performance after external fixation. J Cell Physiol 2008;215:265–275
30. Agheli N, Kabir M, Berni-Canani S, et al. Plasma lipids and fatty acid synthase activity are regulated by short-chain fructo-oligosaccharides in sucrose-fed insulin-resistant rats. J Nutr 1998;128:1283–1288
31. Delbosc S, Paizanis E, Magous R, et al. Involvement of oxidative stress and NADPH oxidase activation in the development of cardiovascular complications in a model of insulin resistance, the fructose-fed rat. Atherosclerosis 2005;179:43–49
32. Nyby MD, Abedi K, Smutko V, Eslami P, Tuck ML. Vascular angiotensin type 1 receptor expression is associated with vascular dysfunction, oxidative stress and inflammation in fructose-fed rats. Hypertens Res 2007;30:451–457
33. Kurata A, Nishizawa H, Kihara S, et al. Blockade of angiotensin II type-1 receptor reduces oxidative stress in adipose tissue and ameliorates adipocytokine dysregulation. Kidney Int 2006;70:1717–1724
34. Santos SH, Braga JF, Mario EG; et al. Improved lipid and glucose metabolism in transgenic rats with increased circulating angiotensin-(1-7). Arterioscler Thromb Vasc Biol 2010;30:953–961
35. Giani JF, Mayer MA, Muñoz MC, et al. Chronic infusion of angiotensin-(1-7) improves insulin resistance and hypertension induced by a high-fructose diet in rats. Am J Physiol Endocrinol Metab 2009;296:E262–E271
36. Zavaroni I, Sander S, Scott S, Reaven GM. Effect of fructose feeding on insulin secretion and insulin action in the rat. Metabolism 1980;29:970–973
37. Tran LT, Yuen VG, McNeill JH. The fructose-fed rat: a review on the mechanisms of fructose-induced insulin resistance and hypertension. Mol Cell Biochem 2009;332:145–159
38. Rayssiguier Y, Gueux E, Nowacki W, Rock E, Mazur A. High fructose consumption combined with low dietary magnesium intake may increase the incidence of the metabolic syndrome by inducing inflammation. Magnes Res 2006;19:237–243
39. Shinozaki K, Ayajiki K, Nishio Y, Sugaya T, Kashiwagi A, Okamura T. Evidence for a causal role of the renin-angiotensin system in vascular dysfunction associated with insulin resistance. Hypertension 2004;43:255–262
40. Seppälä-Lindroos A, Vehkavaara S, Häkkinen AM, et al. Fat accumulation in the liver is associated with defects in insulin suppression of glucose production and serum free fatty acids independent of obesity in normal men. J Clin Endocrinol Metab 2002;87:3023–3028
41. Targher G, Bertolini L, Poli F, et al. Nonalcoholic fatty liver disease and risk of future cardiovascular events among type 2 diabetic patients. Diabetes 2005;54:3541–3546
42. Kanda H, Tateya S, Tamori Y, et al. MCP-1 contributes to macrophage infiltration into adipose tissue, insulin resistance, and hepatic steatosis in obesity. J Clin Invest 2006;116:1494–1505
43. Weisberg SP, Hunter D, Huber R, et al. CCR2 modulates inflammatory and metabolic effects of high-fat feeding. J Clin Invest 2006;116:115–124
44. Cai D, Yuan M, Frantz DF, et al. Local and systemic insulin resistance resulting from hepatic activation of IKK-beta and NF-kappaB. Nat Med 2005;11:183–190
45. Pereira RM, Dos Santos RA, Teixeira MM, et al. The renin-angiotensin system in a rat model of hepatic fibrosis: evidence for a protective role of Angiotensin-(1-7). J Hepatol 2007;46:674–681
46. Kawasaki T, Igarashi K, Koeda T, et al. Rats fed fructose-enriched diets have characteristics of nonalcoholic hepatic steatosis. J Nutr 2009;139:2067–2071
47. Fallo F, Veglio F, Bertello C, et al. Prevalence and characteristics of the metabolic syndrome in primary aldosteronism. J Clin Endocrinol Metab 2006;91:454–459
48. Cooper SA, Whaley-Connell A, Habibi J, et al. Renin-angiotensin-aldosterone system and oxidative stress in cardiovascular insulin resistance. Am J Physiol Heart Circ Physiol 2007;293:H2009–H2023
49. Alexis JD, Wang N, Che W, et al. Bcr kinase activation by angiotensin II inhibits peroxisome-proliferator-activated receptor gamma transcriptional activity in vascular smooth muscle cells. Circ Res 2009;104:69–78
50. Mario EG, Santos SH, Ferreira AV, Bader M, Santos RA, Botion LM. Angiotensin-(1-7) Mas-receptor deficiency decreases peroxisome proliferator-activated receptor gamma expression in adipocytes. Peptides 2012;33:174–177